

A Solid State NMR, Crystallographic and Quantum Chemical
Investigation of Bisphosphonates and Farnesyl Diphosphate Synthase-
Bisphosphonate Complexes

By

Junhong Mao, Sujoy Mukherjee, Yong Zhang, Rong Cao, John M. Sanders,
Yongcheng Song, Yonghui Zhang, Gary A. Meints, Yi Gui Gao, Dushyant
Mukkamala, Michael P. Hudock and Eric Oldfield

Departments of Chemistry and Biophysics, 600 South Mathews Avenue, University of Illinois at
Urbana-Champaign, Urbana, Illinois 61801, USA

SUPPORTING INFORMATION

Full Citations for Abbreviated References Appearing in the Text

45. Frisch, M. J.; Trucks, G. W.; Schlegel, H. B.; Scuseria, G. E.; Robb, M. A.; Cheeseman, J. R.; Zakrzewski, V. G.; Montgomery, J. A., Jr.; Stratmann, R. E.; Burant, J. C.; Dapprich, S.; Millam, J. M.; Daniels, A. D.; Kudin, K. N.; Strain, M. C.; Farkas, O.; Tomasi, J.; Barone, V.; Cossi, M.; Cammi, R.; Mennucci, B.; Pomelli, C.; Adamo, C.; Clifford, S.; Ochterski, J.; Petersson, G. A.; Ayala, P. Y.; Cui, Q.; Morokuma, K.; Malick, D. K.; Rabuck, A. D.; Raghavachari, K.; Foresman, J. B.; Cioslowski, J.; Ortiz, J. V.; Baboul, A. G.; Stefanov, B. B.; Liu, G.; Liashenko, A.; Piskorz, P.; Komaromi, I.; Gomperts, R.; Martin, R. L.; Fox, D. J.; Keith, T.; Al-Laham, M. A.; Peng, C. Y.; Nanayakkara, A.; Gonzalez, C.; Challacombe, M.; Gill, P. M. W.; Johnson, B.; Chen, W.; Wong, M. W.; Andres, J. L.; Gonzalez, C.; Head-Gordon, M.; Replogle, E. S.; Pople, J. A. *Gaussian 98*, Revision A.7; Gaussian, Inc.: Pittsburgh, PA, 1998.
46. Frisch, M. J.; Trucks, G. W.; Schlegel, H. B.; Scuseria, G. E.; Robb, M. A.; Cheeseman, J. R.; Montgomery, J., J. A.; Vreven, T.; Kudin, K. N.; Burant, J. C.; Millam, J. M.; Iyengar, S. S.; Tomasi, J.; Barone, V.; Mennucci, B.; Cossi, M.; Scalmani, G.; Rega, N.; Petersson, G. A.; Nakatsuji, H.; Hada, M.; Ehara, M.; Toyota, K.; Fukuda, R.; Hasegawa, J.; Ishida, M.; Nakajima, T.; Honda, Y.; Kitao, O.; Nakai, H.; Klene, M.; Li, X.; Knox, J. E.; Hratchian, H. P.; Cross, J. B.; Bakken, V.; Adamo, C.; Jaramillo, J.; Gomperts, R.; Stratmann, R. E.; Yazyev, O.; Austin, A. J.; Cammi, R.; Pomelli, C.; Ochterski, J. W.; Ayala, P. Y.; Morokuma, K.; Voth, G. A.; Salvador, P.; Dannenberg, J. J.; Zakrzewski, V. G.; Dapprich, S.; Daniels, A. D.; Strain, M. C.; Farkas, O.; Malick, D. K.; Rabuck, A. D.; Raghavachari, K.; Foresman, J. B.; Ortiz, J. V.; Cui, Q.; Baboul, A. G.; Clifford, S.; Cioslowski, J.; Stefanov, B. B.; Liu, G.; Liashenko, A.; Piskorz, P.; Komaromi, I.; Martin, R. L.; Fox, D. J.; Keith, T.; Al-Laham, M. A.; Peng, C. Y.; Nanayakkara,

A.; Challacombe, M.; Gill, P. M. W.; Johnson, B.; Chen, W.; Wong, M. W.; Gonzalez, C.; Pople, J. A. *Gaussian 03*, Revision B.03; Gaussian, Inc.: Wallingford, CT, 2004.

Supporting Information for Quantum Chemical Calculations

For the pure bisphosphonates, the geometries employed were those we determined crystallographically (see Text). We used a uniform 6-311++G (2d,2p) basis set in all cases, based on an earlier study of related systems¹. Both Hartree-Fock as well as DFT methods were investigated, the latter using the B3LYP functional^{2, 3}. The effects of charge field perturbation were investigated by using a 7.5 Å radius lattice of Merz-Kollman⁴ derived charges. Only the results of the HF/MK calculations are discussed in the Text, since they provided the best correlations with experiment. For the calculations of FPPS-bisphosphonate complexes, we worked primarily on the tertiary complex of FPPS, its inhibitor (risedronate), and one of its substrates, IPP. The x-ray crystallographic structure of one such complex was reported for the *E. coli* FPPS (PDB ID: 1RQJ), and this was used as the starting geometry for geometry optimizations and NMR chemical shielding calculations. The actual bisphosphonate binding site used in the calculations consisted of the 3Mg²⁺ coordination shell and the surrounding hydrogen bond partners and contained 116 atoms. Terminal oxygen atoms in risedronate were investigated with and without protonation as were the terminal oxygens in IPP. The phosphorus atoms and their bonded oxygen atoms were treated with a 6-311++G(2d,2p) basis, while the rest of the atoms were treated with a 6-31G* basis, for both geometry optimization and NMR shielding calculations. A partial geometry optimization on this bisphosphonate cluster was performed by using the DFT method mPW1PW91⁵, in which the coordinates of the two phosphorus atoms and their bonded oxygen atoms, together with the three coordinated Mg atoms, were optimized while the rest of the atoms in the cluster remained in their original positions. For the ¹⁵N NMR

chemical shielding calculations, in addition to calculations performed using single molecule and charge field perturbation approaches, we also carried out a series of calculations using supermolecule clusters, consisting of the central molecule of interest (treated with a 6-311++G(2d,2p) basis) and its hydrogen bonded partner molecules (treated with a 6-31G* basis for the hydrogen bonded atoms and a 3-21G basis for the rest of the atoms).

References

1. Zhang, Y.; Oldfield, E., *J. Phys. Chem. B* **2004**, 108, 19533-19540.
2. Becke, A. D., *J. Chem. Phys.* **1993**, 98, 5648-5652.
3. Lee, C. T.; Yang, W. T.; Parr, R. G., *Phys. Rev. B: Condens. Matter* **1988**, 37, 785-789.
4. Besler, B. H.; Merz, K. M.; Kollman, P. A., *J. Comput. Chem.* **1990**, 11, 431-439.
5. Adamo, C.; Barone, V., *J. Chem. Phys.* **1998**, 108, 664-675.

Supporting Information for Docking Calculations

To calculate atom grid maps used in the docking calculations, we used default interatomic potentials, although the Autogrid source code (the autogrid.h file) was modified so that Autogrid would recognize and correctly type magnesium and phosphorus atoms present in the macromolecules. Manual correction of fragmental volumes and solvation parameters in the macromolecular pdbqs files was also required since the phosphate and diphosphate ligands in the FPPS active sites are non-standard. For the carbon ligand atoms, we used the applicable fragmental volumes from a previous report¹, which is the source for Autodock's built-in fragmental volumes. To determine the fragmental volume for phosphorus, we first used the Molcad module in Sybyl 7.0² to calculate the volumes of phosphate and IPP. Subtracting the

known fragmental volumes for non-phosphorus atoms in phosphate and IPP from the total molecular volumes gave a fragmental volume of $\sim 9.0 \text{ \AA}^3$ for phosphorus, which we then used in all calculations. To calculate the fragmental volume of Mg^{2+} , we simply used the volume of a sphere, taking the radius to be the ionic radius of Mg^{2+} (0.86 Å). For the solvation parameters, we used the Autodock value for Fe^{3+} to approximate that of Mg^{2+} , and for phosphorus we used the Autodock solvation parameter of sulfur. Phosphate oxygens were treated using the Autodock anionic sp^2 values for carboxylate oxygens (from glutamate), while bridging phosphoester oxygens were given the Autodock value for sp^3 hybridized oxygen (from serine). For all carbon atoms, we used the standard carbon Autodock solvation parameter, which is constant for all carbon types. Once these values were established, default settings were used to calculate the atom grid maps, using the centers of mass of the bisphosphonates extracted from each crystal structure as grid centers for the atom grid maps.

Ligand preparation consisted of optimizing the bisphosphonate structures with the Tripos forcefield with the electrostatic component disabled, using the BFGS algorithm and a convergence criterion of $0.001 \text{ kcal}\cdot\text{mol}^{-1}\cdot\text{\AA}^{-1}$. For bisphosphonates with pyridinium side chains, the N-H distance was constrained to 1.02 Å since we obtained unreasonably long N-H bonds (1.5 Å) without constraining this distance. Default settings were used in the docking calculations, with the exceptions of the ga_num_evals (which was increased to 2,500,000) and ga_run (which was increased to 100) parameters.

Electrostatic Potential Calculations. The electrostatic potential for *T. brucei* FPPS was calculated by using the Linearized Poisson-Boltzmann Equation as implemented in the Molcad program in Sybyl 7.0². For protein preparation, all non-protein atoms were removed, with the

exception of the Mg²⁺. Using Sybyl, all hydrogen atoms were added, and Kollman All Atom charges were loaded for the protein, with the magnesium ions being assigned charges of 2.0. The molecular surface of the protein was represented as a Connolly surface, using a probe radius of 1.4 Å and default values for other parameters. For the Poisson-Boltzmann calculation, a step width of 1.0 Å and a border width of 8.0 Å were used. Solute and solvent dielectric values were set to 2.0 and 80.0, respectively, and the ionic strength was taken to be 0.145. Otherwise, default parameters were used.

References

1. Motoc, I.; Marshall, G. R., Van der Waals volume fragmental constants. *Chem. Phys. Lett.* **1985**, 116, (5), 415-419.
2. *Sybyl*, 7.0; Tripos Inc.: St. Louis, 2004.

Table S1. Crystal Data and Structure Refinement for Compound **11**.

Empirical formula	C ₇ H ₁₄ N ₂ O ₇ P ₂	
Formula weight	300.14	
Temperature	193(2) K	
Wavelength	0.71073 Å	
Crystal system	Orthorhombic	
Space group	P b c a	
Unit cell dimensions	a = 17.136(5) Å	α= 90°
	b = 7.522(2) Å	β= 90°
	c = 18.116(6) Å	γ= 90°
Volume	2334.9(12) Å ³	
Z	8	
Density (calculated)	1.708 g cm ⁻³	
Absorption coefficient	0.403 mm ⁻¹	
F(000)	1248	
Crystal size	0.19 x 0.06 x 0.05 mm ³	
Theta range for data collection	2.25 to 25.39°	
Index ranges	-20 ≤ h ≤ 20, -9 ≤ k ≤ 9, -21 ≤ l ≤ 21	
Reflections collected	24391	
Independent reflections	2144 [R(int) = 0.1266]	
Completeness to theta = 25.39°	99.9 %	
Absorption correction	Integration	
Max. and min. transmission	0.9864 and 0.9376	
Refinement method	Full-matrix least-squares on F ²	
Data / restraints / parameters	2144 / 7 / 184	
Goodness-of-fit on F ²	0.998	
Final R indices [I>2σ(I)]	R ₁ = 0.0479, wR ₂ = 0.1077	
R indices (all data)	R ₁ = 0.0815, wR ₂ = 0.1175	
Largest diff. peak and hole	0.300 and -0.324 e.Å ⁻³	

Table S2. Crystal Data and Structure Refinement for Compound **14**.

Empirical formula	C ₁₀ H ₂₃ N ₃ O ₁₁ P ₂		
Formula weight	423.25		
Temperature	193(2) K		
Wavelength	0.71073 Å		
Crystal system	Monoclinic		
Space group	P 21/c		
Unit cell dimensions	a = 8.6608(18) Å	α= 90°	
	b = 14.173(3) Å	β= 102.704(3)°	
	c = 15.231(3) Å	γ = 90°	
Volume	1823.8(6) Å ³		
Z	4		
Density (calculated)	1.541 g cm ⁻³		
Absorption coefficient	0.300 mm ⁻¹		
F(000)	888		
Crystal size	0.54 x 0.18 x 0.13 mm ³		
Theta range for data collection	1.99 to 28.24°		
Index ranges	-11 ≤ h ≤ 11, -18 ≤ k ≤ 18, -20 ≤ l ≤ 20		
Reflections collected	17633		
Independent reflections	4459 [R(int) = 0.0307]		
Completeness to theta = 28.32°	98.8 %		
Absorption correction	Integration		
Max. and min. transmission	0.9641 and 0.8704		
Refinement method	Full-matrix least-squares on F ²		
Data / restraints / parameters	4459 / 18 / 280		
Goodness-of-fit on F ²	1.045		
Final R indices [I>2σ(I)]	R ₁ = 0.0378, wR ₂ = 0.0878		
R indices (all data)	R ₁ = 0.0581, wR ₂ = 0.0951		
Largest diff. peak and hole	0.383 and -0.335 e.Å ⁻³		

Table S3. Crystal Data and Structure Refinement for Compound **15**.

Empirical formula	C ₅ H ₉ NO ₆ P ₂ S		
Formula weight	273.13		
Temperature	193(2) K		
Wavelength	0.71073 Å		
Crystal system	Triclinic		
Space group	P -1		
Unit cell dimensions	a = 7.208(6) Å	α = 109.700(12)°	
	b = 8.465(6) Å	β = 106.731(12)°	
	c = 8.911(7) Å	γ = 97.664(13)°	
Volume	473.9(6) Å ³		
Z	2		
Density (calculated)	1.914 g cm ⁻³		
Absorption coefficient	0.688 mm ⁻¹		
F(000)	280		
Crystal size	0.16 x 0.14 x 0.09 mm ³		
Theta range for data collection	2.60 to 27.50°		
Index ranges	-9 ≤ h ≤ 9, -10 ≤ k ≤ 10, -11 ≤ l ≤ 11		
Reflections collected	5519		
Independent reflections	2105 [R(int) = 0.0324]		
Completeness to theta = 28.32°	96.8 %		
Absorption correction	Integration		
Max. and min. transmission	0.9464 and 0.9072		
Refinement method	Full-matrix least-squares on F ²		
Data / restraints / parameters	2105 / 3 / 148		
Goodness-of-fit on F ²	1.061		
Final R indices [I>2σ(I)]	R ₁ = 0.0322, wR ₂ = 0.0838		
R indices (all data)	R ₁ = 0.0404, wR ₂ = 0.0879		
Largest diff. peak and hole	0.436 and -0.374 e.Å ⁻³		

Table S4. Crystal Data and Structure Refinement for Compound **16**.

Empirical formula	C ₅ H ₁₆ N ₂ O ₁₀ P ₂		
Formula weight	326.14		
Temperature	193(2) K		
Wavelength	0.71073 Å		
Crystal system	Triclinic		
Space group	P -1		
Unit cell dimensions	a = 6.822(9) Å	α = 114.984(16)°	
	b = 9.561(12) Å	β = 94.397(17)°	
	c = 10.523(13) Å	γ = 97.901(18)°	
Volume	609.3(13) Å ³		
Z	2		
Density (calculated)	1.788 g cm ⁻³		
Absorption coefficient	0.411 mm ⁻¹		
F(000)	340		
Crystal size	0.40 x 0.38 x 0.06 mm ³		
Theta range for data collection	3.05 to 28.01°		
Index ranges	-9 ≤ h ≤ 9, -12 ≤ k ≤ 12, -13 ≤ l ≤ 13		
Reflections collected	6947		
Independent reflections	2891 [R(int) = 0.0271]		
Completeness to theta = 28.32°	98.4 %		
Absorption correction	Integration		
Max. and min. transmission	0.9761 and 0.8628		
Refinement method	Full-matrix least-squares on F ²		
Data / restraints / parameters	2891 / 33 / 203		
Goodness-of-fit on F ²	1.078		
Final R indices [I>2σ(I)]	R ₁ = 0.0321, wR ₂ = 0.0853		
R indices (all data)	R ₁ = 0.0386, wR ₂ = 0.0892		
Largest diff. peak and hole	0.405 and -0.500 e.Å ⁻³		

Table S5. Crystal Data and Structure Refinement Compound **17**.

Empirical formula	C ₄ H ₇ NO ₆ P ₂ S ₂		
Formula weight	291.17		
Temperature	193(2) K		
Wavelength	0.71073 Å		
Crystal system	Triclinic		
Space group	P -1		
Unit cell dimensions	a = 7.325(2) Å	α = 68.240(5)°	
	b = 13.776(3) Å	β = 85.371(5)°	
	c = 8.972(3) Å	γ = 82.608°	
Volume	469.8(3) Å ³		
Z	2		
Density (calculated)	2.058 g cm ⁻³		
Absorption coefficient	0.915 mm ⁻¹		
F(000)	296		
Crystal size	0.32 x 0.30 x 0.08 mm ³		
Theta range for data collection	2.45 to 28.27°		
Index ranges	-9 ≤ h ≤ 9, -10 ≤ k ≤ 10, -11 ≤ l ≤ 11		
Reflections collected	5815		
Independent reflections	2252 [R(int) = 0.0335]		
Completeness to theta = 28.32°	96.8 %		
Absorption correction	Integration		
Max. and min. transmission	0.9299 and 0.7627		
Refinement method	Full-matrix least-squares on F ²		
Data / restraints / parameters	2252 / 3 / 148		
Goodness-of-fit on F ²	1.045		
Final R indices [I>2σ(I)]	R ₁ = 0.0312, wR ₂ = 0.0819		
R indices (all data)	R ₁ = 0.0390, wR ₂ = 0.0882		
Largest diff. peak and hole	0.480 and -0.391 e.Å ⁻³		

Table S6. Crystal Data and Structure Refinement for Compound **18**.

Empirical formula	C ₄ H ₉ N ₃ O ₇ P ₂		
Formula weight	273.08		
Temperature	193(2) K		
Wavelength	0.71073 Å		
Crystal system	Monoclinic		
Space group	P 21/c		
Unit cell dimensions	a = 7.524(3) Å	α = 90°	
	b = 13.975(5) Å	β = 103.647(7)°	
	c = 9.437(4) Å	γ = 90°	
Volume	964.3(7) Å ³		
Z	4		
Density (calculated)	1.881 g cm ⁻³		
Absorption coefficient	0.480 mm ⁻¹		
F(000)	560		
Crystal size	0.32 x 0.20 x 0.07 mm ³		
Theta range for data collection	2.66 to 28.32°		
Index ranges	-8 ≤ h ≤ 9, -18 ≤ k ≤ 18, -12 ≤ l ≤ 12		
Reflections collected	10242		
Independent reflections	2385 [R(int) = 0.0359]		
Completeness to theta = 28.32°	99.2 %		
Absorption correction	Integration		
Max. and min. transmission	0.9722 and 0.8818		
Refinement method	Full-matrix least-squares on F ²		
Data / restraints / parameters	2385 / 3 / 158		
Goodness-of-fit on F ²	1.036		
Final R indices [I>2σ(I)]	R ₁ = 0.0345, wR ₂ = 0.0893		
R indices (all data)	R ₁ = 0.0440, wR ₂ = 0.0943		
Largest diff. peak and hole	0.452 and -0.460 e.Å ⁻³		

Table S7. Crystal Data and Structure Refinement for Compound **19**.

Empirical formula	C ₅ H ₁₅ NO ₆ P ₂		
Formula weight	247.12		
Temperature	193(2) K		
Wavelength	0.71073 Å		
Crystal system	Monoclinic		
Space group	P 21/c		
Unit cell dimensions	a = 9.715(4) Å	α = 90°	
	b = 21.430(10) Å	β = 93.575(8)°	
	c = 10.023(5) Å	γ = 90°	
Volume	2082.6(16) Å ³		
Z	8		
Density (calculated)	1.576 g cm ⁻³		
Absorption coefficient	0.423 mm ⁻¹		
F(000)	1040		
Crystal size	0.60 x 0.12 x 0.03 mm ³		
Theta range for data collection	2.10 to 25.38°		
Index ranges	-11 ≤ h ≤ 11, -25 ≤ k ≤ 25, -12 ≤ l ≤ 12		
Reflections collected	21296		
Independent reflections	3828 [R(int) = 0.0497]		
Completeness to theta = 25.38°	99.9 %		
Absorption correction	Integration		
Max. and min. transmission	0.9881 and 0.8581		
Refinement method	Full-matrix least-squares on F ²		
Data / restraints / parameters	3828 / 10 / 285		
Goodness-of-fit on F ²	1.031		
Final R indices [I>2σ(I)]	R ₁ = 0.0348, wR ₂ = 0.0851		
R indices (all data)	R ₁ = 0.0460, wR ₂ = 0.0896		
Largest diff. peak and hole	0.413 and -0.345 e.Å ⁻³		

Table S8. Crystal Data and Structure Refinement for Compound **20a**.

Empirical formula	C ₅ H ₁₈ NNaO ₆ P ₂		
Formula weight	309.16		
Temperature	193(2) K		
Wavelength	0.71073 Å		
Crystal system	Triclinic		
Space group	P -1		
Unit cell dimensions	a = 6.258(3) Å	α = 85.515(9)°	
	b = 6.413(3) Å	β = 84.998(9)°	
	c = 17.221(9) Å	γ = 71.069(9)°	
Volume	650.3(6) Å ³		
Z	2		
Density (calculated)	1.579 g cm ⁻³		
Absorption coefficient	0.386 mm ⁻¹		
F(000)	324		
Crystal size	0.65 x 0.08 x 0.02 mm ³		
Theta range for data collection	2.38 to 25.41°		
Index ranges	-7 ≤ h ≤ 7, -7 ≤ k ≤ 7, -20 ≤ l ≤ 20		
Reflections collected	6715		
Independent reflections	2391 [R(int) = 0.0577]		
Completeness to theta = 25.38°	99.5 %		
Absorption correction	Integration		
Max. and min. transmission	0.9921 and 0.8466		
Refinement method	Full-matrix least-squares on F ²		
Data / restraints / parameters	2391 / 342 / 230		
Goodness-of-fit on F ²	1.060		
Final R indices [I>2σ(I)]	R ₁ = 0.0534, wR ₂ = 0.1183		
R indices (all data)	R ₁ = 0.0837, wR ₂ = 0.1284		
Largest diff. peak and hole	0.631 and -0.387 e.Å ⁻³		

Table S9. Crystal Data and Structure Refinement for Compound **20b**.

Empirical formula	C ₈ H ₁₉ NO ₆ P ₂		
Formula weight	287.18		
Temperature	193(2) K		
Wavelength	0.71073 Å		
Crystal system	Monoclinic		
Space group	P 21/c		
Unit cell dimensions	a = 11.540(3) Å	α = 90°	
	b = 6.5177(16) Å	β = 91.214(5)°	
	c = 16.752(4) Å	γ = 90°	
Volume	1259.7(5) Å ³		
Z	4		
Density (calculated)	1.514 g cm ⁻³		
Absorption coefficient	0.361 mm ⁻¹		
F(000)	608		
Crystal size	0.33 x 0.16 x 0.03 mm ³		
Theta range for data collection	1.76 to 25.36°		
Index ranges	-13 ≤ h ≤ 13, -7 ≤ k ≤ 7, -20 ≤ l ≤ 20		
Reflections collected	13187		
Independent reflections	2301 [R(int) = 0.1343]		
Completeness to theta = 25.36°	100.0 %		
Absorption correction	Integration		
Max. and min. transmission	0.9886 and 0.9195		
Refinement method	Full-matrix least-squares on F ²		
Data / restraints / parameters	2301 / 5 / 169		
Goodness-of-fit on F ²	0.967		
Final R indices [I>2σ(I)]	R ₁ = 0.0573, wR ₂ = 0.0938		
R indices (all data)	R ₁ = 0.1160, wR ₂ = 0.1078		
Largest diff. peak and hole	0.416 and -0.357 e.Å ⁻³		

Table S10. Data collection and refinement statistics for *T. brucei* FPPS +**11**

<u>Crystal</u>	FPPS + 11
Data Collection	
Space group	C2
Unit-cell parameters	
a, b, c (Å)	133.214,119.55,62.438
β(°)	111.927
X-ray source	BNL-X12C *
Wavelength (Å)	1.1
Resolution (Å)	30-2.20 (2.28-2.20)
Total reflections	276,805
Unique	41,878(2595)
Completeness (%)	91.0 (56.5)
Rmerge	0.073 (0.424)
I/σI	10.1
Multiplicity	6.6(3.5)
Refinement Statistics (30-2.28 Å)	
R-all (%)	21.75
R-work (%)	21.70
R-free (%)	24.44
RMSD	
Bond length (Å)	0.005
Bond angles (°)	1.741
No. of atoms	
Protein	5833
Ligand	2 bisphosphonates
Solvent(water)	358
Magnesium ion	6
B average(Å ²)	34.43 (protein main and side chain atoms) 32.38 (compound 11 and Mg ²⁺)

Table S11. Geometry of the partially optimized risedronate binding site.

HEADER	PROTEIN
COMPND	C:\babel\t.ent
AUTHOR	GENERATED BY BABEL 1.6
HETATM	1 H UNK 1 -4.081 1.003 0.650
HETATM	2 H UNK 1 -4.942 2.177 -0.108
HETATM	3 C UNK 1 -5.632 1.769 1.791
HETATM	4 N UNK 1 -5.007 1.367 0.489
HETATM	5 H UNK 1 -5.018 2.559 2.248
HETATM	6 H UNK 1 -6.629 2.178 1.569
HETATM	7 H UNK 1 -5.575 0.659 0.046
HETATM	8 H UNK 1 -5.703 0.917 2.468
HETATM	9 H 9 4.261 4.568 0.419
HETATM	10 H 10 3.082 3.543 -0.074
HETATM	11 H 11 2.851 5.162 -0.204
HETATM	12 C 12 4.124 4.411 -1.651
HETATM	13 N 13 3.533 4.423 -0.263
HETATM	14 H 14 3.319 4.265 -2.385
HETATM	15 H 15 4.595 5.389 -1.830
HETATM	16 H 16 4.856 3.608 -1.744
HETATM	17 O 17 -0.119 2.327 -3.681
HETATM	18 H 18 -0.677 1.437 -3.661
HETATM	19 H 19 0.898 2.100 -3.808
HETATM	20 O 20 -3.466 -3.898 -0.390
HETATM	21 H 21 -4.008 -3.993 0.504
HETATM	22 H 22 -2.854 -4.742 -0.519
HETATM	23 C 23 -0.005 -4.284 -3.340
HETATM	24 C 24 -1.199 -3.787 -2.561
HETATM	25 O 25 -1.070 -2.761 -1.835
HETATM	26 O 26 -2.311 -4.368 -2.589
HETATM	27 H 27 0.255 -3.547 -4.114
HETATM	28 H 28 0.841 -4.382 -2.644
HETATM	29 O 29 2.390 -2.459 -2.101
HETATM	30 H 30 2.104 -3.366 -2.547
HETATM	31 H 31 3.020 -2.653 -1.284
HETATM	32 C 32 0.965 -4.200 2.033
HETATM	33 C 33 0.306 -3.299 1.008
HETATM	34 O 34 1.043 -2.616 0.264
HETATM	35 O 35 -0.931 -3.209 0.888
HETATM	36 H 36 1.996 -3.857 2.205
HETATM	37 H 37 0.401 -4.115 2.973
HETATM	38 MG 38 0.645 -1.418 -1.276
HETATM	39 O 39 0.069 2.742 1.524
HETATM	40 H 40 0.865 2.971 1.990
HETATM	41 C 41 0.583 0.384 2.008
HETATM	42 H 42 1.550 0.675 2.444
HETATM	43 H 43 0.679 -0.586 1.496
HETATM	44 C 44 -0.364 0.164 3.169
HETATM	45 C 45 -0.344 -1.098 3.760
HETATM	46 H 46 0.318 -1.866 3.377
HETATM	47 C 47 -1.177 -1.370 4.844
HETATM	48 H 48 -1.171 -2.348 5.312
HETATM	49 C 49 -2.012 -0.369 5.310
HETATM	50 H 50 -2.667 -0.566 6.151
HETATM	51 N 51 -2.019 0.844 4.734
HETATM	52 H 52 -2.629 1.552 5.090

HETATM	53	C	53	-1.224	1.126	3.689
HETATM	54	H	54	-1.252	2.115	3.247
HETATM	55	O	55	0.256	-0.302	-3.132
HETATM	56	H	56	-0.385	-0.842	-3.763
HETATM	57	H	57	1.156	-0.102	-3.635
HETATM	58	C	58	-0.679	7.017	0.681
HETATM	59	C	59	0.080	5.810	0.217
HETATM	60	O	60	1.314	5.844	0.236
HETATM	61	O	61	-0.469	4.772	-0.215
HETATM	62	H	62	-1.747	6.768	0.755
HETATM	63	H	63	-0.309	7.291	1.680
HETATM	64	O	64	0.948	4.952	-2.584
HETATM	65	H	65	1.066	5.717	-1.876
HETATM	66	H	66	0.540	5.350	-3.466
HETATM	67	MG	67	-0.295	3.405	-1.702
HETATM	68	MG	68	-2.250	-2.166	-0.328
HETATM	69	O	69	-3.508	-1.235	-1.706
HETATM	70	H	70	-4.350	-1.846	-1.852
HETATM	71	H	71	-2.997	-1.121	-2.617
HETATM	72	O	72	-3.457	-1.424	1.355
HETATM	73	H	73	-4.173	-2.153	1.594
HETATM	74	H	74	-3.942	-0.534	1.082
HETATM	75	H	75	-0.543	7.841	-0.019
HETATM	76	H	76	-0.231	-5.243	-3.808
HETATM	77	H	77	0.975	-5.231	1.681
HETATM	78	P	78	1.683	1.498	-0.190
HETATM	79	P	79	-1.339	0.973	0.067
HETATM	80	O	80	-1.526	1.927	-1.106
HETATM	81	O	81	-1.044	-0.478	-0.393
HETATM	82	O	82	-2.484	1.020	1.074
HETATM	83	O	83	1.876	0.074	-0.692
HETATM	84	O	84	1.439	2.507	-1.305
HETATM	85	O	85	2.800	2.001	0.731
HETATM	86	C	86	0.224	1.443	0.959
HETATM	87	O	87	-2.123	4.337	-2.626
HETATM	88	H	88	-2.552	4.987	-1.921
HETATM	89	H	89	-2.821	3.599	-2.890
HETATM	90	C	90	7.568	-0.753	1.814
HETATM	91	N	91	6.301	-1.223	1.275
HETATM	92	C	92	5.210	-0.483	1.152
HETATM	93	N	93	4.104	-1.046	0.690
HETATM	94	N	94	5.199	0.810	1.500
HETATM	95	H	95	7.375	-0.118	2.691
HETATM	96	H	96	8.149	-1.630	2.132
HETATM	97	H	97	6.250	-2.204	0.965
HETATM	98	H	98	4.337	1.363	1.395
HETATM	99	H	99	6.053	1.251	1.872
HETATM	100	H	100	3.246	-0.486	0.588
HETATM	101	H	101	4.103	-2.043	0.432
HETATM	102	H	102	8.112	-0.183	1.061
HETATM	103	C	103	-7.553	-2.213	0.524
HETATM	104	C	104	-6.582	-1.935	-0.590
HETATM	105	O	105	-6.257	-0.745	-0.826
HETATM	106	O	106	-6.063	-2.845	-1.268
HETATM	107	H	107	-7.196	-3.076	1.106
HETATM	108	H	108	-7.580	-1.330	1.180

HETATM 109 H 109 -8.543 -2.425 0.122
 HETATM 110 C 110 5.228 -5.635 -0.832
 HETATM 111 C 111 5.426 -4.209 -0.461
 HETATM 112 O 112 6.416 -3.910 0.252
 HETATM 113 O 113 4.643 -3.325 -0.824
 HETATM 114 H 114 5.774 -5.843 -1.763
 HETATM 115 H 115 5.647 -6.257 -0.027
 HETATM 116 H 116 4.168 -5.849 -0.972
 CONECT 1 4
 CONECT 2 4
 CONECT 3 4 5 6 8
 CONECT 4 1 2 3 7
 CONECT 5 3
 CONECT 6 3
 CONECT 7 4
 CONECT 8 3
 CONECT 9 13
 CONECT 10 13
 CONECT 11 13
 CONECT 12 13 14 15 16
 CONECT 13 9 10 11 12
 CONECT 14 12
 CONECT 15 12
 CONECT 16 12
 CONECT 17 18 19 67
 CONECT 18 17
 CONECT 19 17
 CONECT 20 21 22 68
 CONECT 21 20
 CONECT 22 20
 CONECT 23 24 27 28 76
 CONECT 24 23 25 26
 CONECT 25 24 68 38
 CONECT 26 24
 CONECT 27 23
 CONECT 28 23
 CONECT 29 30 31 38
 CONECT 30 29
 CONECT 31 29
 CONECT 32 33 36 37 77
 CONECT 33 32 34 35
 CONECT 34 33 38
 CONECT 35 33 68
 CONECT 36 32
 CONECT 37 32
 CONECT 38 29 34 55 81 83 25
 CONECT 39 40 86
 CONECT 40 39
 CONECT 41 42 43 44 86
 CONECT 42 41
 CONECT 43 41
 CONECT 44 41 45 53
 CONECT 45 44 46 47
 CONECT 46 45
 CONECT 47 45 48 49
 CONECT 48 47

CONECT 49 47 50 51
CONECT 50 49
CONECT 51 49 52 53
CONECT 52 51
CONECT 53 44 51 54
CONECT 54 53
CONECT 55 38 56 57
CONECT 56 55
CONECT 57 55
CONECT 58 59 62 63 75
CONECT 59 58 60 61
CONECT 60 59
CONECT 61 59 67
CONECT 62 58
CONECT 63 58
CONECT 64 65 66 67
CONECT 65 64
CONECT 66 64
CONECT 67 61 64 80 84 87 17
CONECT 68 20 25 35 69 72 81
CONECT 69 68 70 71
CONECT 70 69
CONECT 71 69
CONECT 72 68 73 74
CONECT 73 72
CONECT 74 72
CONECT 75 58
CONECT 76 23
CONECT 77 32
CONECT 78 83 84 85 86
CONECT 79 80 81 82 86
CONECT 80 67 79
CONECT 81 38 79 68
CONECT 82 79
CONECT 83 78 38
CONECT 84 67 78
CONECT 85 78
CONECT 86 39 41 78 79
CONECT 87 88 89 67
CONECT 88 87
CONECT 89 87
CONECT 90 91 95 96 102
CONECT 91 90 92 97
CONECT 92 91 93 94
CONECT 93 92 100 101
CONECT 94 92 98 99
CONECT 95 90
CONECT 96 90
CONECT 97 91
CONECT 98 94
CONECT 99 94
CONECT 100 93
CONECT 101 93
CONECT 102 90
CONECT 103 104 107 108 109
CONECT 104 103 105 106

CONECT 105 104
CONECT 106 104
CONECT 107 103
CONECT 108 103
CONECT 109 103
CONECT 110 111 114 115 116
CONECT 111 110 112 113
CONECT 112 111
CONECT 113 111
CONECT 114 110
CONECT 115 110
CONECT 116 110
END

Table S12. Geometry of the partially optimized IPP binding site (fully deprotonated).

HETATM	1	O	1	15.505	17.649	0.655
HETATM	2	H1	2	15.532	18.589	0.376
HETATM	3	H2	3	16.410	17.329	0.655
HETATM	4	HCA	4	12.189	17.713	-0.992
HETATM	5	C	5	12.688	17.037	-1.671
HETATM	6	O	6	12.221	15.901	-1.822
HETATM	7	N	7	13.776	17.465	-2.305
HETATM	8	CA	8	14.378	16.698	-3.397
HETATM	9	H	9	14.140	18.401	-2.118
HETATM	10	HA	10	13.578	16.096	-3.828
HETATM	11	H	11	15.199	16.075	-3.042
HETATM	12	H	12	14.764	17.383	-4.152
HETATM	13	O	13	11.540	21.193	-2.775
HETATM	14	H1	14	11.540	22.153	-2.775
HETATM	15	H2	15	12.033	21.014	-1.944
HETATM	16	O	16	12.191	23.940	-0.324
HETATM	17	H1	17	12.191	24.900	-0.324
HETATM	18	H2	18	12.905	23.695	-0.924
HETATM	19	HCD	19	14.902	19.845	-5.736
HETATM	20	CE	20	15.503	20.635	-5.285
HETATM	21	NZ	21	14.661	21.571	-4.488
HETATM	22	1HE	22	16.240	20.166	-4.634
HETATM	23	2HE	23	15.994	21.223	-6.060
HETATM	24	1HZ	24	15.257	22.293	-3.977
HETATM	25	2HZ	25	14.001	22.032	-5.098
HETATM	26	3HZ	26	14.200	21.070	-3.685
HETATM	27	O	27	13.596	24.842	-2.548
HETATM	28	H1	28	13.596	25.802	-2.548
HETATM	29	H2	29	14.515	24.532	-2.662
HETATM	30	HCD	30	21.653	20.245	1.352
HETATM	31	NE	31	21.626	21.189	0.993
HETATM	32	CZ	32	20.623	21.574	0.213
HETATM	33	NH1	33	20.591	22.816	-0.258
HETATM	34	NH2	34	19.642	20.736	-0.106
HETATM	35	HE	35	22.362	21.840	1.227
HETATM	36	1HH1	36	21.330	23.462	-0.021
HETATM	37	2HH1	37	19.828	23.108	-0.851
HETATM	38	1HH2	38	19.655	19.790	0.248
HETATM	39	2HH2	39	18.804	21.058	-0.657
HETATM	40	P11	40	14.399	20.851	-0.647
HETATM	41	O14	41	12.964	21.229	-0.353
HETATM	42	O12	42	15.064	20.176	0.535
HETATM	43	O13	43	14.619	20.291	-2.038
HETATM	44	O10	44	15.298	22.327	-0.734
HETATM	45	P7	45	16.534	22.606	-1.666
HETATM	46	O8	46	17.609	21.554	-1.761
HETATM	47	O9	47	16.061	23.250	-2.952
HETATM	48	O6	48	17.340	23.712	-0.808
HETATM	49	C5	49	16.665	24.901	-0.520
HETATM	50	C4	50	17.539	25.684	0.451
HETATM	51	C2	51	18.923	25.954	-0.086
HETATM	52	C1	52	19.970	25.641	0.637
HETATM	53	C3	53	19.094	26.613	-1.425

HETATM 54 H 54 15.694 24.716 -0.061
 HETATM 55 H 55 16.532 25.478 -1.435
 HETATM 56 H 56 17.657 25.068 1.342
 HETATM 57 H 57 17.054 26.629 0.696
 HETATM 58 H 58 19.839 25.193 1.611
 HETATM 59 H 59 20.964 25.831 0.259
 HETATM 60 H 60 18.621 27.595 -1.410
 HETATM 61 H 61 18.628 25.998 -2.195
 HETATM 62 H 62 20.156 26.724 -1.642
 HETATM 63 O 63 17.228 19.008 -1.948
 HETATM 64 H1 64 17.256 19.983 -1.937
 HETATM 65 H2 65 18.133 18.688 -1.948
 HETATM 66 HCG 66 9.853 21.028 1.108
 HETATM 67 CD 67 10.202 20.545 2.021
 HETATM 68 NE 68 11.633 20.275 1.973
 HETATM 69 CZ 69 12.305 19.671 2.947
 HETATM 70 NH1 70 11.688 19.269 4.048
 HETATM 71 NH2 71 13.608 19.464 2.826
 HETATM 72 1HD 72 9.986 21.214 2.854
 HETATM 73 2HD 73 9.703 19.585 2.156
 HETATM 74 HE 74 12.173 20.629 1.145
 HETATM 75 1HH1 75 10.695 19.422 4.151
 HETATM 76 2HH1 76 12.213 18.811 4.779
 HETATM 77 1HH2 77 14.134 19.716 1.950
 HETATM 78 2HH2 78 14.114 19.004 3.569
 CONECT 1 2 3
 CONECT 2 1
 CONECT 3 1
 CONECT 4 5
 CONECT 5 4 6 7
 CONECT 6 5
 CONECT 7 5 9 8
 CONECT 8 7 10 11 12
 CONECT 9 7
 CONECT 10 8
 CONECT 11 8
 CONECT 12 8
 CONECT 13 14 15
 CONECT 14 13
 CONECT 15 13
 CONECT 16 17 18
 CONECT 17 16
 CONECT 18 16
 CONECT 19 20
 CONECT 20 19 21 22 23
 CONECT 21 20 24 25 26
 CONECT 22 20
 CONECT 23 20
 CONECT 24 21
 CONECT 25 21
 CONECT 26 21
 CONECT 27 28 29
 CONECT 28 27
 CONECT 29 27
 CONECT 30 31
 CONECT 31 30 32 35

```
CONECT 32 31 33 34
CONECT 33 32 36 37
CONECT 34 32 38 39
CONECT 35 31
CONECT 36 33
CONECT 37 33
CONECT 38 34
CONECT 39 34
CONECT 40 41 42 43 44
CONECT 41 40
CONECT 42 40
CONECT 43 40
CONECT 44 40 45
CONECT 45 44 46 47 48
CONECT 46 45
CONECT 47 45
CONECT 48 45 49
CONECT 49 48 50 54 55
CONECT 50 49 51 56 57
CONECT 51 50 52 53
CONECT 52 51 58 59
CONECT 53 51 60 61 62
CONECT 54 49
CONECT 55 49
CONECT 56 50
CONECT 57 50
CONECT 58 52
CONECT 59 52
CONECT 60 53
CONECT 61 53
CONECT 62 53
CONECT 63 64 65
CONECT 64 63
CONECT 65 63
CONECT 66 67
CONECT 67 66 68 72 73
CONECT 68 67 69 74
CONECT 69 68 70 71
CONECT 70 69 75 76
CONECT 71 69 77 78
CONECT 72 67
CONECT 73 67
CONECT 74 68
CONECT 75 70
CONECT 76 70
CONECT 77 71
CONECT 78 71
END
```

Table S13. Geometry of the partially optimized IPP binding site (mono- protonated at O13).

HETATM	1	O	1	15.505	17.649	0.655
HETATM	2	H1	2	15.579	18.620	0.649
HETATM	3	H2	3	16.410	17.329	0.655
HETATM	4	HCA	4	12.189	17.713	-0.992
HETATM	5	C	5	12.688	17.037	-1.671
HETATM	6	O	6	12.221	15.901	-1.822
HETATM	7	N	7	13.776	17.465	-2.305
HETATM	8	CA	8	14.378	16.698	-3.397
HETATM	9	H	9	14.070	18.413	-2.142
HETATM	10	HA	10	13.578	16.096	-3.828
HETATM	11	H	11	15.199	16.075	-3.042
HETATM	12	H	12	14.764	17.383	-4.152
HETATM	13	O	13	11.540	21.193	-2.775
HETATM	14	H1	14	11.540	22.153	-2.775
HETATM	15	H2	15	11.962	20.996	-1.918
HETATM	16	O	16	12.191	23.940	-0.324
HETATM	17	H1	17	12.191	24.900	-0.324
HETATM	18	H2	18	12.839	23.743	-1.012
HETATM	19	HCD	19	14.902	19.845	-5.736
HETATM	20	CE	20	15.503	20.635	-5.285
HETATM	21	NZ	21	14.661	21.571	-4.488
HETATM	22	1HE	22	16.240	20.166	-4.634
HETATM	23	2HE	23	15.994	21.223	-6.060
HETATM	24	1HZ	24	15.242	22.295	-3.955
HETATM	25	2HZ	25	14.001	22.032	-5.098
HETATM	26	3HZ	26	14.106	21.072	-3.780
HETATM	27	O	27	13.596	24.842	-2.548
HETATM	28	H1	28	13.596	25.802	-2.548
HETATM	29	H2	29	14.515	24.555	-2.696
HETATM	30	HCD	30	21.653	20.245	1.352
HETATM	31	NE	31	21.626	21.189	0.993
HETATM	32	CZ	32	20.623	21.574	0.213
HETATM	33	NH1	33	20.591	22.816	-0.258
HETATM	34	NH2	34	19.642	20.736	-0.106
HETATM	35	HE	35	22.362	21.840	1.227
HETATM	36	1HH1	36	21.330	23.462	-0.021
HETATM	37	2HH1	37	19.828	23.108	-0.851
HETATM	38	1HH2	38	19.655	19.790	0.248
HETATM	39	2HH2	39	18.819	21.055	-0.648
HETATM	40	P11	40	14.576	20.898	-0.426
HETATM	41	O14	41	13.108	21.096	-0.358
HETATM	42	O12	42	15.308	20.359	0.760
HETATM	43	O13	43	14.910	20.039	-1.744
HETATM	44	O10	44	15.266	22.323	-0.843
HETATM	45	P7	45	16.563	22.640	-1.730
HETATM	46	O8	46	17.568	21.530	-1.830
HETATM	47	O9	47	16.057	23.272	-2.997
HETATM	48	O6	48	17.332	23.694	-0.823
HETATM	49	C5	49	16.665	24.901	-0.520
HETATM	50	C4	50	17.539	25.684	0.451
HETATM	51	C2	51	18.923	25.954	-0.086
HETATM	52	C1	52	19.970	25.641	0.637
HETATM	53	C3	53	19.094	26.613	-1.425
HETATM	54	H	54	15.694	24.716	-0.061
HETATM	55	H	55	16.532	25.478	-1.435

HETATM	56	H	56	17.657	25.068	1.342
HETATM	57	H	57	17.054	26.629	0.696
HETATM	58	H	58	19.839	25.193	1.611
HETATM	59	H	59	20.964	25.831	0.259
HETATM	60	H	60	18.621	27.595	-1.410
HETATM	61	H	61	18.628	25.998	-2.195
HETATM	62	H	62	20.156	26.724	-1.642
HETATM	63	O	63	17.228	19.008	-1.948
HETATM	64	H1	64	17.336	19.987	-2.042
HETATM	65	H2	65	18.133	18.688	-1.948
HETATM	66	HCG	66	9.853	21.028	1.108
HETATM	67	CD	67	10.202	20.545	2.021
HETATM	68	NE	68	11.633	20.275	1.973
HETATM	69	CZ	69	12.305	19.671	2.947
HETATM	70	NH1	70	11.688	19.269	4.048
HETATM	71	NH2	71	13.608	19.464	2.826
HETATM	72	1HD	72	9.986	21.214	2.854
HETATM	73	2HD	73	9.703	19.585	2.156
HETATM	74	HE	74	12.166	20.604	1.155
HETATM	75	1HH1	75	10.695	19.422	4.151
HETATM	76	2HH1	76	12.213	18.811	4.779
HETATM	77	1HH2	77	14.162	19.805	2.027
HETATM	78	2HH2	78	14.114	19.004	3.569
HETATM	79	H	79	15.656	19.423	-1.590
CONECT	1	2	3			
CONECT	2	1				
CONECT	3	1				
CONECT	4	5				
CONECT	5	4	6	7		
CONECT	6	5				
CONECT	7	5	9	8		
CONECT	8	7	10	11	12	
CONECT	9	7				
CONECT	10	8				
CONECT	11	8				
CONECT	12	8				
CONECT	13	14	15			
CONECT	14	13				
CONECT	15	13				
CONECT	16	17	18			
CONECT	17	16				
CONECT	18	16				
CONECT	19	20				
CONECT	20	19	21	22	23	
CONECT	21	20	24	25	26	
CONECT	22	20				
CONECT	23	20				
CONECT	24	21				
CONECT	25	21				
CONECT	26	21				
CONECT	27	28	29			
CONECT	28	27				
CONECT	29	27				
CONECT	30	31				
CONECT	31	30	32	35		
CONECT	32	31	33	34		

```
CONECT 33 32 36 37
CONECT 34 32 38 39
CONECT 35 31
CONECT 36 33
CONECT 37 33
CONECT 38 34
CONECT 39 34
CONECT 40 41 42 43 44
CONECT 41 40
CONECT 42 40
CONECT 43 40
CONECT 44 40 45
CONECT 45 44 46 47 48
CONECT 46 45
CONECT 47 45
CONECT 48 45 49
CONECT 49 48 50 54 55
CONECT 50 49 51 56 57
CONECT 51 50 52 53
CONECT 52 51 58 59
CONECT 53 51 60 61 62
CONECT 54 49
CONECT 55 49
CONECT 56 50
CONECT 57 50
CONECT 58 52
CONECT 59 52
CONECT 60 53
CONECT 61 53
CONECT 62 53
CONECT 63 64 65
CONECT 64 63
CONECT 65 63
CONECT 66 67
CONECT 67 66 68 72 73
CONECT 68 67 69 74
CONECT 69 68 70 71
CONECT 70 69 75 76
CONECT 71 69 77 78
CONECT 72 67
CONECT 73 67
CONECT 74 68
CONECT 75 70
CONECT 76 70
CONECT 77 71
CONECT 78 71
CONECT 79 43
END
```

Table S14. Geometry of the partially optimized IPP binding site (mono- protonated at O14).

HETATM	1	O	1	15.505	17.649	0.655
HETATM	2	H1	2	15.549	18.545	0.283
HETATM	3	H2	3	16.410	17.329	0.655
HETATM	4	HCA	4	12.189	17.713	-0.992
HETATM	5	C	5	12.688	17.037	-1.671
HETATM	6	O	6	12.221	15.901	-1.822
HETATM	7	N	7	13.776	17.465	-2.305
HETATM	8	CA	8	14.378	16.698	-3.397
HETATM	9	H	9	14.136	18.387	-2.094
HETATM	10	HA	10	13.578	16.096	-3.828
HETATM	11	H	11	15.199	16.075	-3.042
HETATM	12	H	12	14.764	17.383	-4.152
HETATM	13	O	13	11.540	21.193	-2.775
HETATM	14	H1	14	11.540	22.153	-2.775
HETATM	15	H2	15	12.340	20.932	-2.285
HETATM	16	O	16	12.191	23.940	-0.324
HETATM	17	H1	17	12.191	24.900	-0.324
HETATM	18	H2	18	12.508	23.823	-1.243
HETATM	19	HCD	19	14.902	19.845	-5.736
HETATM	20	CE	20	15.503	20.635	-5.285
HETATM	21	NZ	21	14.661	21.571	-4.488
HETATM	22	1HE	22	16.240	20.166	-4.634
HETATM	23	2HE	23	15.994	21.223	-6.060
HETATM	24	1HZ	24	15.248	22.304	-4.000
HETATM	25	2HZ	25	14.001	22.032	-5.098
HETATM	26	3HZ	26	14.176	21.093	-3.703
HETATM	27	O	27	13.596	24.842	-2.548
HETATM	28	H1	28	13.596	25.802	-2.548
HETATM	29	H2	29	14.515	24.524	-2.657
HETATM	30	HCD	30	21.653	20.245	1.352
HETATM	31	NE	31	21.626	21.189	0.993
HETATM	32	CZ	32	20.623	21.574	0.213
HETATM	33	NH1	33	20.591	22.816	-0.258
HETATM	34	NH2	34	19.642	20.736	-0.106
HETATM	35	HE	35	22.362	21.840	1.227
HETATM	36	1HH1	36	21.330	23.462	-0.021
HETATM	37	2HH1	37	19.828	23.108	-0.851
HETATM	38	1HH2	38	19.655	19.790	0.248
HETATM	39	2HH2	39	18.838	21.045	-0.680
HETATM	40	P11	40	14.481	21.053	-0.533
HETATM	41	O14	41	13.207	21.688	0.189
HETATM	42	O12	42	15.095	20.171	0.486
HETATM	43	O13	43	14.126	20.560	-1.902
HETATM	44	O10	44	15.414	22.368	-0.706
HETATM	45	P7	45	16.605	22.675	-1.736
HETATM	46	O8	46	17.605	21.581	-1.901
HETATM	47	O9	47	16.001	23.322	-2.952
HETATM	48	O6	48	17.382	23.734	-0.844
HETATM	49	C5	49	16.665	24.901	-0.520
HETATM	50	C4	50	17.539	25.684	0.451
HETATM	51	C2	51	18.923	25.954	-0.086
HETATM	52	C1	52	19.970	25.641	0.637
HETATM	53	C3	53	19.094	26.613	-1.425
HETATM	54	H	54	15.694	24.716	-0.061
HETATM	55	H	55	16.532	25.478	-1.435

HETATM	56	H	56	17.657	25.068	1.342
HETATM	57	H	57	17.054	26.629	0.696
HETATM	58	H	58	19.839	25.193	1.611
HETATM	59	H	59	20.964	25.831	0.259
HETATM	60	H	60	18.621	27.595	-1.410
HETATM	61	H	61	18.628	25.998	-2.195
HETATM	62	H	62	20.156	26.724	-1.642
HETATM	63	O	63	17.228	19.008	-1.948
HETATM	64	H1	64	17.293	19.977	-2.015
HETATM	65	H2	65	18.133	18.688	-1.948
HETATM	66	HCG	66	9.853	21.028	1.108
HETATM	67	CD	67	10.202	20.545	2.021
HETATM	68	NE	68	11.633	20.275	1.973
HETATM	69	CZ	69	12.305	19.671	2.947
HETATM	70	NH1	70	11.688	19.269	4.048
HETATM	71	NH2	71	13.608	19.464	2.826
HETATM	72	1HD	72	9.986	21.214	2.854
HETATM	73	2HD	73	9.703	19.585	2.156
HETATM	74	HE	74	12.186	20.705	1.229
HETATM	75	1HH1	75	10.695	19.422	4.151
HETATM	76	2HH1	76	12.213	18.811	4.779
HETATM	77	1HH2	77	14.130	19.673	1.960
HETATM	78	2HH2	78	14.114	19.004	3.569
HETATM	79	H	79	12.986	22.641	0.098
CONECT	1	2	3			
CONECT	2	1				
CONECT	3	1				
CONECT	4	5				
CONECT	5	4	6	7		
CONECT	6	5				
CONECT	7	5	9	8		
CONECT	8	7	10	11	12	
CONECT	9	7				
CONECT	10	8				
CONECT	11	8				
CONECT	12	8				
CONECT	13	14	15			
CONECT	14	13				
CONECT	15	13				
CONECT	16	17	18			
CONECT	17	16				
CONECT	18	16				
CONECT	19	20				
CONECT	20	19	21	22	23	
CONECT	21	20	24	25	26	
CONECT	22	20				
CONECT	23	20				
CONECT	24	21				
CONECT	25	21				
CONECT	26	21				
CONECT	27	28	29			
CONECT	28	27				
CONECT	29	27				
CONECT	30	31				
CONECT	31	30	32	35		
CONECT	32	31	33	34		

```
CONECT 33 32 36 37
CONECT 34 32 38 39
CONECT 35 31
CONECT 36 33
CONECT 37 33
CONECT 38 34
CONECT 39 34
CONECT 40 41 42 43 44
CONECT 41 40
CONECT 42 40
CONECT 43 40
CONECT 44 40 45
CONECT 45 44 46 47 48
CONECT 46 45
CONECT 47 45
CONECT 48 45 49
CONECT 49 48 50 54 55
CONECT 50 49 51 56 57
CONECT 51 50 52 53
CONECT 52 51 58 59
CONECT 53 51 60 61 62
CONECT 54 49
CONECT 55 49
CONECT 56 50
CONECT 57 50
CONECT 58 52
CONECT 59 52
CONECT 60 53
CONECT 61 53
CONECT 62 53
CONECT 63 64 65
CONECT 64 63
CONECT 65 63
CONECT 66 67
CONECT 67 66 68 72 73
CONECT 68 67 69 74
CONECT 69 68 70 71
CONECT 70 69 75 76
CONECT 71 69 77 78
CONECT 72 67
CONECT 73 67
CONECT 74 68
CONECT 75 70
CONECT 76 70
CONECT 77 71
CONECT 78 71
CONECT 79 41
END
```

Table S15. Geometry of the partially optimized IPP binding site (mono- protonated at O12).

HETATM	1	O	1	15.505	17.649	0.655
HETATM	2	H1	2	15.577	18.599	0.502
HETATM	3	H2	3	16.410	17.329	0.655
HETATM	4	HCA	4	12.189	17.713	-0.992
HETATM	5	C	5	12.688	17.037	-1.671
HETATM	6	O	6	12.221	15.901	-1.822
HETATM	7	N	7	13.776	17.465	-2.305
HETATM	8	CA	8	14.378	16.698	-3.397
HETATM	9	H	9	14.085	18.417	-2.147
HETATM	10	HA	10	13.578	16.096	-3.828
HETATM	11	H	11	15.199	16.075	-3.042
HETATM	12	H	12	14.764	17.383	-4.152
HETATM	13	O	13	11.540	21.193	-2.775
HETATM	14	H1	14	11.540	22.153	-2.775
HETATM	15	H2	15	12.274	20.935	-2.198
HETATM	16	O	16	12.191	23.940	-0.324
HETATM	17	H1	17	12.191	24.900	-0.324
HETATM	18	H2	18	12.821	23.769	-1.038
HETATM	19	HCD	19	14.902	19.845	-5.736
HETATM	20	CE	20	15.503	20.635	-5.285
HETATM	21	NZ	21	14.661	21.571	-4.488
HETATM	22	1HE	22	16.240	20.166	-4.634
HETATM	23	2HE	23	15.994	21.223	-6.060
HETATM	24	1HZ	24	15.253	22.314	-4.022
HETATM	25	2HZ	25	14.001	22.032	-5.098
HETATM	26	3HZ	26	14.186	21.087	-3.699
HETATM	27	O	27	13.596	24.842	-2.548
HETATM	28	H1	28	13.596	25.802	-2.548
HETATM	29	H2	29	14.513	24.557	-2.718
HETATM	30	HCD	30	21.653	20.245	1.352
HETATM	31	NE	31	21.626	21.189	0.993
HETATM	32	CZ	32	20.623	21.574	0.213
HETATM	33	NH1	33	20.591	22.816	-0.258
HETATM	34	NH2	34	19.642	20.736	-0.106
HETATM	35	HE	35	22.362	21.840	1.227
HETATM	36	1HH1	36	21.330	23.462	-0.021
HETATM	37	2HH1	37	19.828	23.108	-0.851
HETATM	38	1HH2	38	19.655	19.790	0.248
HETATM	39	2HH2	39	18.839	21.047	-0.678
HETATM	40	P11	40	14.719	20.906	-0.656
HETATM	41	O14	41	13.730	21.020	0.439
HETATM	42	O12	42	15.987	20.148	-0.044
HETATM	43	O13	43	14.328	20.361	-1.997
HETATM	44	O10	44	15.343	22.381	-0.920
HETATM	45	P7	45	16.623	22.710	-1.834
HETATM	46	O8	46	17.599	21.577	-1.985
HETATM	47	O9	47	16.108	23.385	-3.070
HETATM	48	O6	48	17.372	23.719	-0.858
HETATM	49	C5	49	16.665	24.901	-0.520
HETATM	50	C4	50	17.539	25.684	0.451
HETATM	51	C2	51	18.923	25.954	-0.086
HETATM	52	C1	52	19.970	25.641	0.637
HETATM	53	C3	53	19.094	26.613	-1.425
HETATM	54	H	54	15.694	24.716	-0.061
HETATM	55	H	55	16.532	25.478	-1.435

HETATM	56	H	56	17.657	25.068	1.342
HETATM	57	H	57	17.054	26.629	0.696
HETATM	58	H	58	19.839	25.193	1.611
HETATM	59	H	59	20.964	25.831	0.259
HETATM	60	H	60	18.621	27.595	-1.410
HETATM	61	H	61	18.628	25.998	-2.195
HETATM	62	H	62	20.156	26.724	-1.642
HETATM	63	O	63	17.228	19.008	-1.948
HETATM	64	H1	64	17.317	19.943	-2.259
HETATM	65	H2	65	18.133	18.688	-1.948
HETATM	66	HCG	66	9.853	21.028	1.108
HETATM	67	CD	67	10.202	20.545	2.021
HETATM	68	NE	68	11.633	20.275	1.973
HETATM	69	CZ	69	12.305	19.671	2.947
HETATM	70	NH1	70	11.688	19.269	4.048
HETATM	71	NH2	71	13.608	19.464	2.826
HETATM	72	1HD	72	9.986	21.214	2.854
HETATM	73	2HD	73	9.703	19.585	2.156
HETATM	74	HE	74	12.206	20.649	1.207
HETATM	75	1HH1	75	10.695	19.422	4.151
HETATM	76	2HH1	76	12.213	18.811	4.779
HETATM	77	1HH2	77	14.082	19.823	2.000
HETATM	78	2HH2	78	14.114	19.004	3.569
HETATM	79	H	79	16.493	19.638	-0.731
CONECT	1	2	3			
CONECT	2	1				
CONECT	3	1				
CONECT	4	5				
CONECT	5	4	6	7		
CONECT	6	5				
CONECT	7	5	9	8		
CONECT	8	7	10	11	12	
CONECT	9	7				
CONECT	10	8				
CONECT	11	8				
CONECT	12	8				
CONECT	13	14	15			
CONECT	14	13				
CONECT	15	13				
CONECT	16	17	18			
CONECT	17	16				
CONECT	18	16				
CONECT	19	20				
CONECT	20	19	21	22	23	
CONECT	21	20	24	25	26	
CONECT	22	20				
CONECT	23	20				
CONECT	24	21				
CONECT	25	21				
CONECT	26	21				
CONECT	27	28	29			
CONECT	28	27				
CONECT	29	27				
CONECT	30	31				
CONECT	31	30	32	35		
CONECT	32	31	33	34		

```
CONECT 33 32 36 37
CONECT 34 32 38 39
CONECT 35 31
CONECT 36 33
CONECT 37 33
CONECT 38 34
CONECT 39 34
CONECT 40 41 42 43 44
CONECT 41 40
CONECT 42 40
CONECT 43 40
CONECT 44 40 45
CONECT 45 44 46 47 48
CONECT 46 45
CONECT 47 45
CONECT 48 45 49
CONECT 49 48 50 54 55
CONECT 50 49 51 56 57
CONECT 51 50 52 53
CONECT 52 51 58 59
CONECT 53 51 60 61 62
CONECT 54 49
CONECT 55 49
CONECT 56 50
CONECT 57 50
CONECT 58 52
CONECT 59 52
CONECT 60 53
CONECT 61 53
CONECT 62 53
CONECT 63 64 65
CONECT 64 63
CONECT 65 63
CONECT 66 67
CONECT 67 66 68 72 73
CONECT 68 67 69 74
CONECT 69 68 70 71
CONECT 70 69 75 76
CONECT 71 69 77 78
CONECT 72 67
CONECT 73 67
CONECT 74 68
CONECT 75 70
CONECT 76 70
CONECT 77 71
CONECT 78 71
CONECT 79 42
END
```

Table S16. ^{13}C and ^{15}N NMR chemical shieldings in a model of **11**^a.

$\angle \text{N}^\gamma\text{-C}^\delta\text{-N}^\varepsilon\text{-C}^\zeta$ (degrees)	Nucleus ^b	E(au)	σ^{calc} (ppm)
0	N^γ	-341.24990	188.9
	N^ε		117.8
	C^δ		29.1
	C^ζ		50.5
30	N^γ	-341.24714	191.5
	N^ε		112.3
	C^δ		26.3
	C^ζ		50.5
60	N^γ	-341.24009	199.3
	N^ε		97.7
	C^δ		23.0
	C^ζ		50.4
90	N^γ	-341.23234	217.9
	N^ε		76.1
	C^δ		23.6
	C^ζ		47.4
120	N^γ	-341.24184	204.3
	N^ε		93.0
	C^δ		22.5
	C^ζ		48.1
150	N^γ	-341.24848	192.0
	N^ε		113.6
	C^δ		25.9
	C^ζ		51.2
180	N^γ	-341.25151	187.3
	N^ε		121.2
	C^δ		29.0
	C^ζ		52.2

^a The molecular structure (trans, NH⁺) of **11** in the crystal structure was used and truncated at the α -carbon, then optimized with the orientation of $\angle \text{N}^\gamma\text{-C}^\delta\text{-N}^\varepsilon\text{-C}^\zeta$ fixed at 0, 30, 60, 90, 120, 150, 180 degrees.

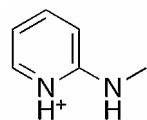
**11 model**

Figure Captions

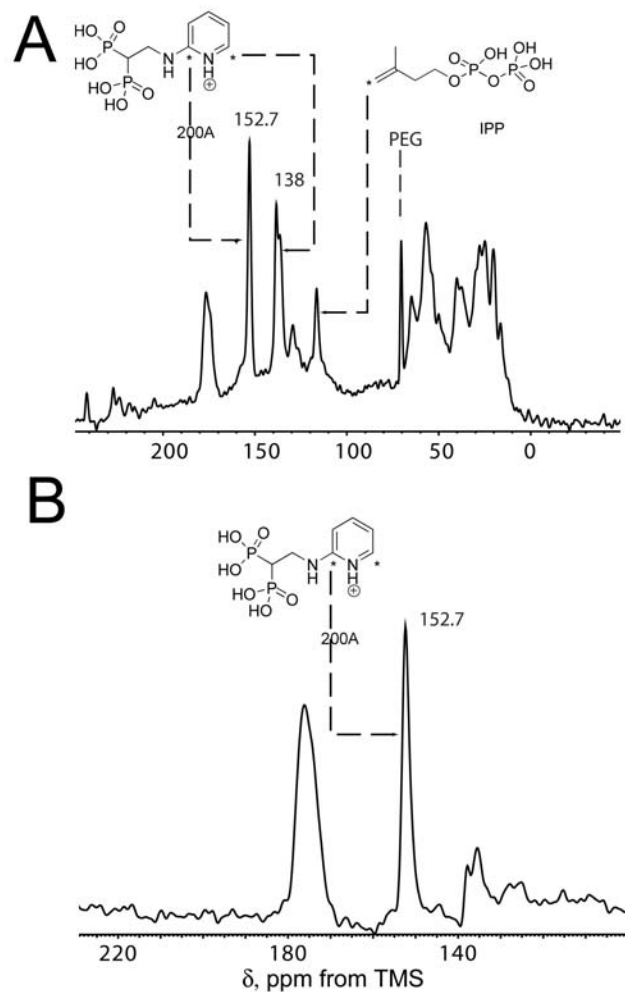
Figure S1. 125 MHz ^{13}C MAS NMR spectra of $^{13}\text{C}_2$ -labeled **11** plus [4- $^{13}\text{C}_1$]-labeled IPP bound to *T. brucei* FPPS in the presence of Mg^{2+} . **A**, proton-decoupled spectrum; **B**, interrupted decoupling spectrum showing [2- ^{13}C]-**11** (quaternary) carbon resonance. PEG = polyethylene glycol resonance.

Figure S2. Histograms of crystallographic P-O bond lengths in bisphosphonates. **A**, The black symbols are for the pure bisphosphonate model compounds. The red symbols are for risedronate in the *E. coli* FPPS/risedronate/IPP Mg complex and the green symbols are the risedronate P-O bond lengths in the complex after QM geometry optimization; **B**, P-O bond lengths for bisphosphonates in PDB structures 1RQJ, 1YV5, 1YQ7, 1ZW5, 1YHL, 1YHM, and 2EWG.

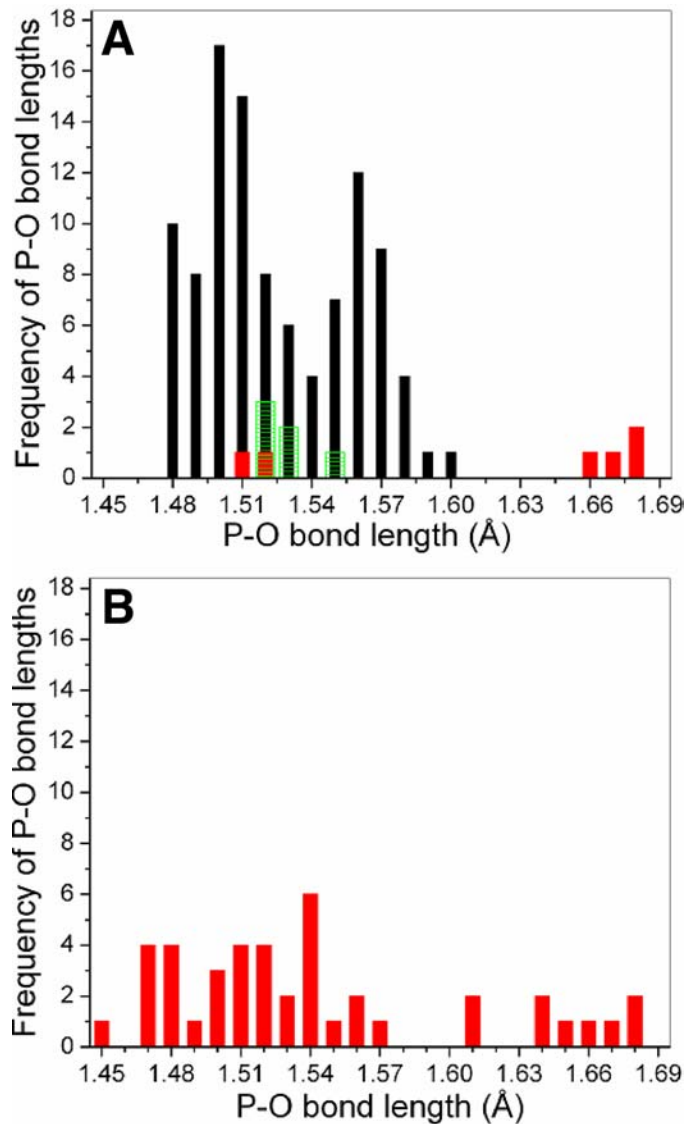
Figure S3. 145.62 MHz ^{31}P NMR spectra of selected bisphosphonates. **A**, **18**, 4.5 kHz MAS; **B**, **13**, 4.5 kHz MAS; **C**, **19**, 4.5 kHz MAS; **D**, **19**, solution NMR spectrum; **E**, 2D ^{31}P - ^{31}P RFDR spectra of **19** at a spinning frequency of 12.0 kHz and a mix time of 25ms; **F**, as **E**, but at a mix time of 100ms.

Figure S4. Geometry-optimized molecular clusters of risedronate (top) and IPP (bottom) sites.

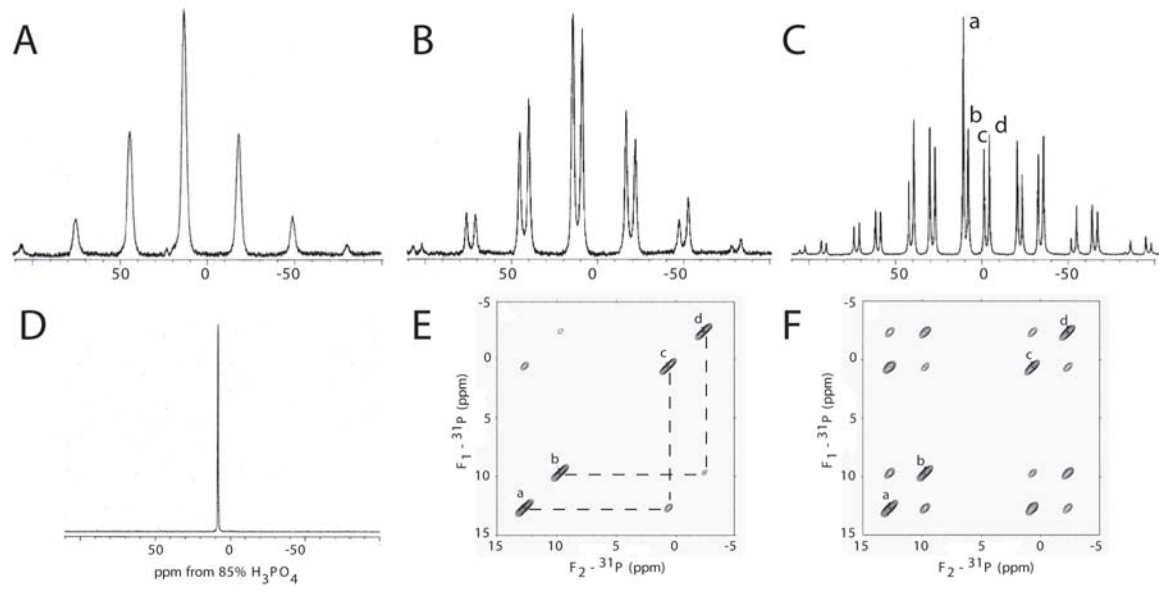
Figure S5. Poisson-Boltzmann electrostatic potential mapped to the Connolly surface of *T. brucei* FPPS. The potential ranges from 0.0 (purple) to +50.0 (red) kcal/mol. The red regions are due to the Mg^{2+} ions (cyan spheres), and the blue region near the minodronate side chain corresponds to the locations of the oxygen atoms that are thought to stabilize the positive charge in the bisphosphonate side chain. Also shown is minodronate, with the NH^+ feature being in close proximity to the negative electrostatic potential surface of the protein. Uncharged side chains would not be expected to interact favorably with the protein.



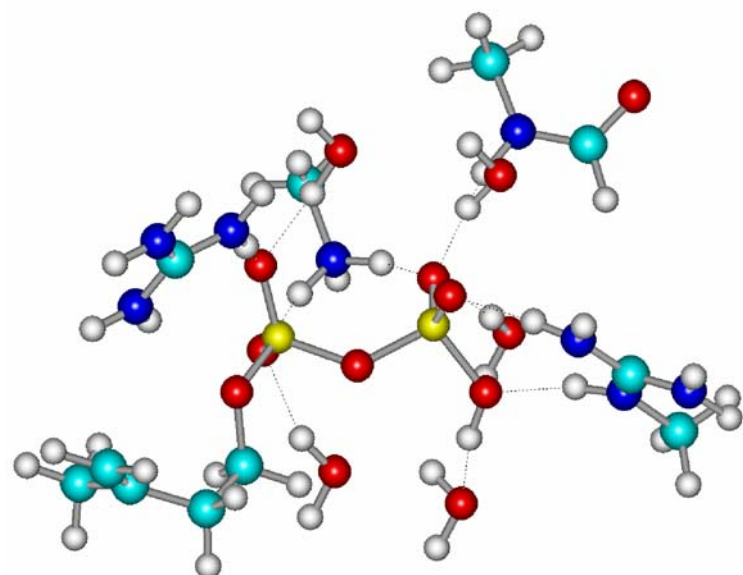
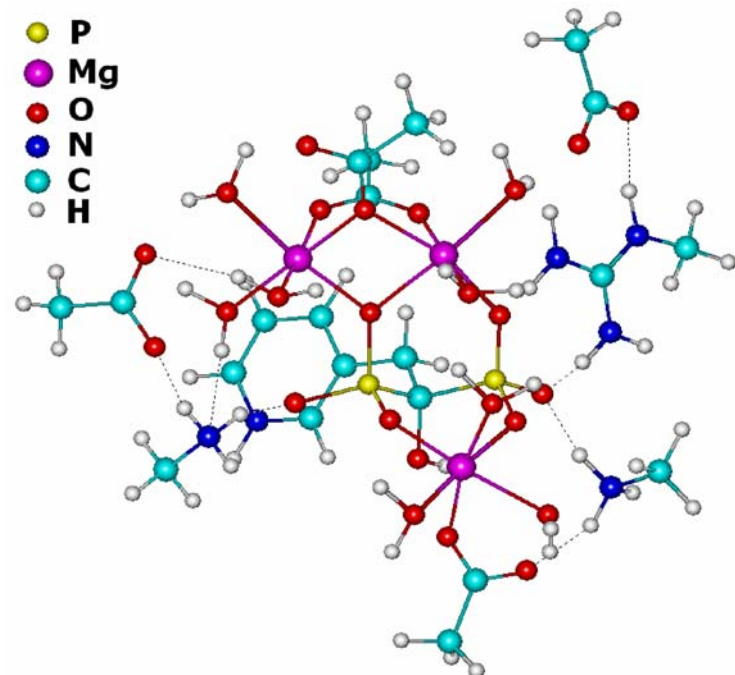
Mao et al., Figure S1



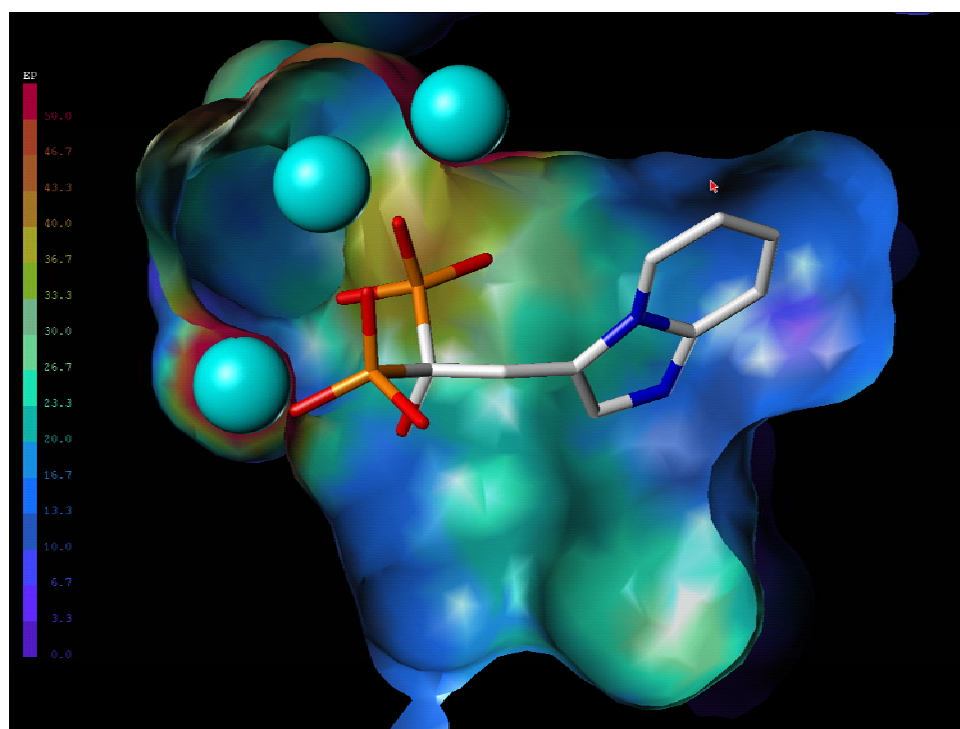
Mao et al., Figure S2



Mao et al., Figure S3



Mao et al., Figure S4



Mao et al., Figure S5